Supporting Information

Air Exposure Induced Recombination in PTB7:$PC_{71}BM$ Solar Cells

Stuart A. J. Thomson, Stephen C. Hogg, Ifor D. W. Samuel, and David J. Keeble

Table S1. Solar cell parameters of pristine and air exposed cells with and without DIO

Exposure	DIO	PCE (%)	FF (%)	J_{SC} (mA cm^{-2})	V_{OC}(V)
Pristine	Yes	6.1	64.9	13.0	0.73
Air Exposed	Yes	1.7	42.6	6.5	0.59
Pristine	No	2.2	45.9	6.6	0.72
Air Exposed	No	1.5	42.8	5.3	0.66

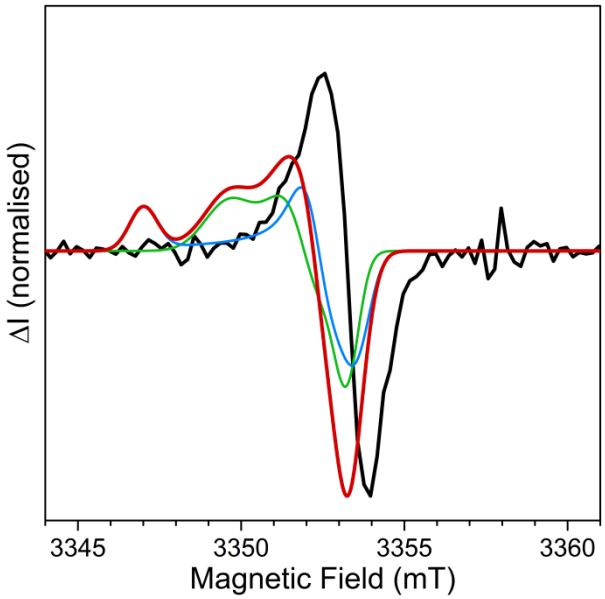

Figure S1. Comparison of 94 GHz experimental EDMR spectrum (black) with simulated EPR light induced EPR spectrum (red) comprising positive (green) and negative (blue) polarons on PTB7:$PC_{71}BM$. The simulated spectrum uses the principal values reported by Niklas et al.[1]

Proton Spin Satellites

At high microwave powers two satellite peaks of the 2.0022(2) resonance become apparent (Figure S2a). The microwave power dependence of the central and satellite lines is shown in Figure S2b. It can be seen that the intensity dependence of the central line breaks from linearity at low microwave powers indicating that it has entered the saturation regime while the satellite intensity remains linear over the measured range. This behaviour is characteristic of nuclear

spin flip satellites. A spin flip satellite occurs when the electron (hole) spin and a neighbouring nuclear spin both flip during resonance. As this is a forbidden transition the spin flip satellites do not enter saturation and their relative intensity therefore increases with respect to the central line as the microwave power is increased. Spin flip satellites are separated from the central line by the nuclear Zeeman interaction,

$$\Delta B_{sat} = \frac{g_N \mu_N B}{g_e \mu_B},$$

where g_N is the g-factor of a proton, which has the value 5.5, and g_e = 2.0023. The satellites were simulated (orange line) using Lorentzian lineshapes and a centre-satellite spacing given by the above equation. As can be seen from Figure S2a, the simulated spectra is in excellent agreement to the experimental spectrum which confirms that the satellites are due to proton spin flips. The satellite intensity follows a B^{-2} dependence which prevents the observation of the spin flip satellites at higher microwave frequencies, and hence magnetic fields.

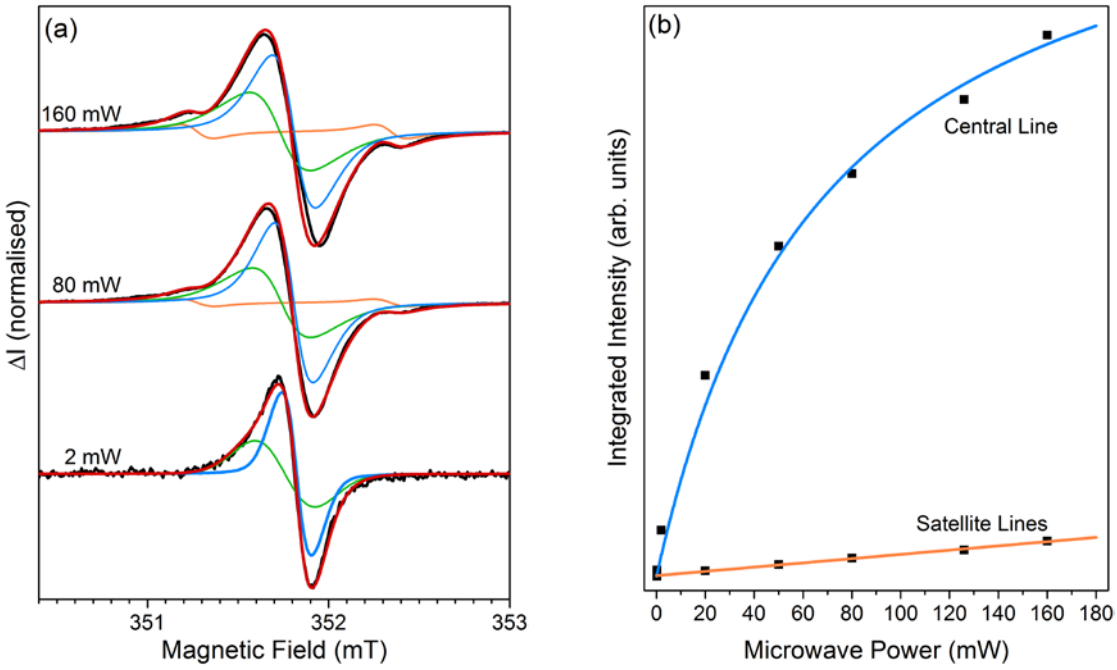

Figure S2. (a) Variation of 9.8 GHz EDMR spectra of PTB7:$PC_{71}BM$ with microwave power. Spectra were recorded using a field modulation amplitude of 0.05 mT. Experimental spectra are shown in black, the total simulation in red and the underlying components in blue, green and orange. (b) Microwave power dependence of the integrated intensity of the 2.0022 line and its satellites in PTB7:$PC_{71}BM$ blend.

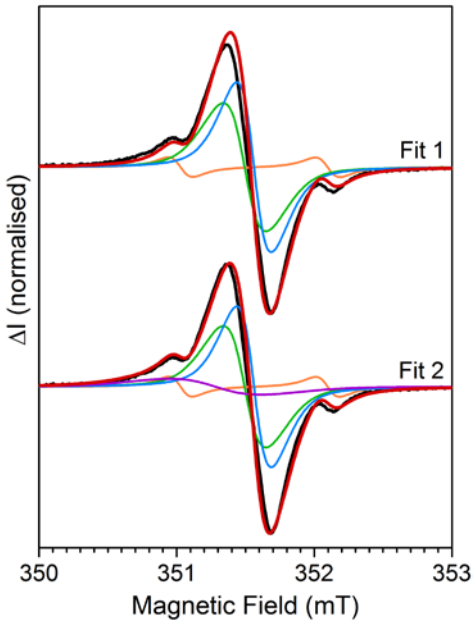

Figure S3. EDMR spectra of PTB7:$PC_{71}BM$ recorded under short circuit conditions with white light illumination at high microwave power (200 mW) using a field modulation amplitude of 0.05 mT. Experimental spectra are shown in black, the total simulation in red and the underlying components in blue, green and purple. At high microwave power the two component fit (plus satellites) poorly reproduces the experimental spectrum (Fit 1). The addition of a third broad component centred on 2.0038(3) improves the accuracy of the fit (Fit 2).

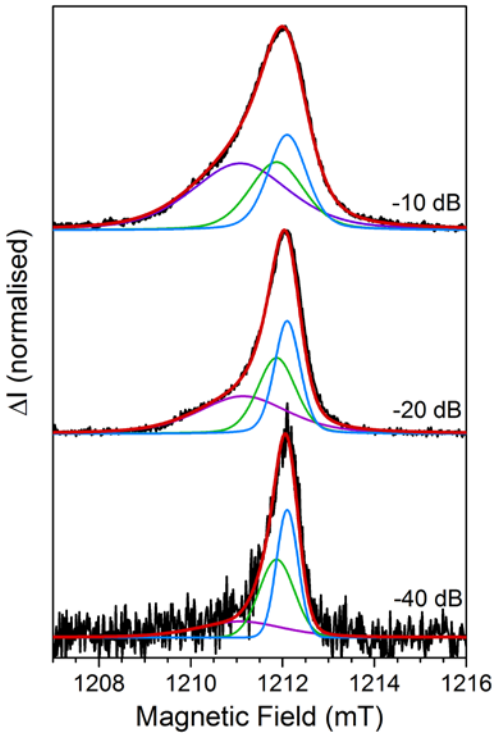

Figure S4. 34 GHz Pulse EDMR spectra of PTB7:$PC_{71}BM$. Experimental spectra are shown in black, the total simulation in red and the underlying components in blue, green and purple. As the pulse power is lowered (increasing attenuation in dB) the relative intensity of the broad component centred on 2.0038(3) (purple) decreases.

Injection Spectra

Injection of carriers into the blend results in the appearance of additional features on the low field side of the spectrum. To explore the influence of injection voltage we recorded EDMR spectra over a range of forward bias voltages and microwave powers, a selection of which are shown in **Figure S5**. The forward bias spectra can be simulated approximately by including two additional distributions centred at 2.0037(3) (purple) and 2.0074(2) (orange) with FWHM of 1.02(5) mT and 0.35(3) mT and Voigtian and Gaussian lineshapes respectively. These distributions are additional to those of the spin-pair and its associated spin flip satellites which are collectively shown here in blue. The relative intensity of these additional distributions increases with respect to the spin-pair as the forward bias voltage is increased. The distribution centred on 2.0037(3) has similar g-value and linewidth as the short lived broad distribution identified in the pEDMR spectrum at high microwave powers suggesting it corresponds to the same species.

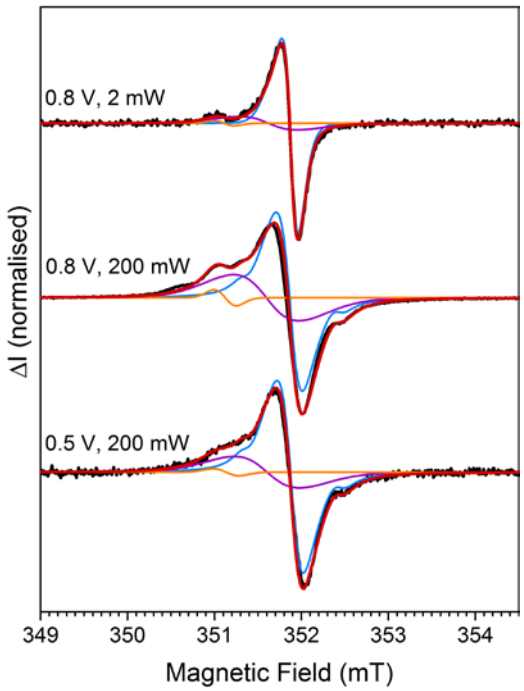

Figure S5. EDMR spectra of ambipolar PTB7:$PC_{71}BM$ cells recorded under forward bias in the dark using a field modulation amplitude of 0.05 mT. Experimental spectra are shown in black, the total simulation in red, the spin-pair in blue and the injection induced features in purple and orange.

It can also be noted that the relative change in modulation phase required to achieve signal maximum when measuring the cwEDMR spectra at short circuit (photogenerated) and under forward bias (injection in the dark) was approximately 10-30°. As the phase of the cwEDMR signal did not invert the EDMR response at resonance in the injection regime it must also be due a current decrease. This provides further evidence that the same mechanism is responsible for the primary EDMR signal (blue) in both regimes, and it is valid to compare magnitudes.

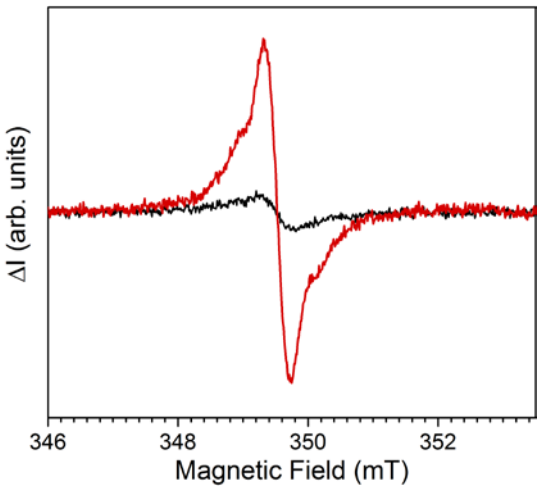

Figure S6. EDMR spectra of $PC_{71}BM$ cells recorded under forward bias in the dark using a field modulation amplitude of 0.3 mT. Air exposed spectra are in red and pristine in black.

$PC_{71}BM$ with DIO

Attempts were made to fabricate neat $PC_{71}BM$ films processed using DIO. However, the film quality becomes extremely poor when even a small volume of DIO (< 1 %) is added to the solution. The resulting cells were electrically unstable, preventing EDMR measurements to be obtained.

The research data supporting this publication can be accessed at DOI http://dx.doi.org/10.17630/cab0e1d8-d12a-4f73-a692-01dcd8aae516

1. J. Niklas, K. L. Mardis, B. P. Banks, G. M. Grooms, A. Sperlich, V. Dyakonov, S. Beaupre, M. Leclerc, T. Xu, L. P. Yu and O. G. Poluektov, *Phys. Chem. Chem. Phys.*, 2013, **15**, 9562-9574.